Journal of Scientific & Industrial Research
Vol. 81, January 2022, pp. 21-31

# New Mathematical Models of Thin Layer Solar Drying of Carrots

Melike Sultan Karasu Asnaz
Department of Industrial Engineering, Balikesir University, Balikesir, Turkey

*Received 23 April 2021; revised 27 December 2021; accepted 27 December 2021*

Drying behavior of julienne and cylindrical cuts of carrot *(var. Danvers)* using a solar dryer for both forced and natural convection mode have been undertaken. Sixteen solar drying experiments were carried out in July 2020, which received an average of 11.6 hours of daylight per day. Instant weight change, temperature, relative humidity and solar radiation were monitored, recorded and analysed. Overall uncertainty caused by various instruments, calibration, and reading was calculated. Then, the moisture content of different sliced carrots at different drying airflow and temperatures were converted into moisture ratio and then fitted against drying time. A total of eight mathematical models, including three new models, as well as five mathematical models commonly used in the literature, were compared to find the most fitted solar drying curve based on the coefficient of determination ($R^2$), the Root Mean Square Error (RMSE), and the mean square of the deviations ($\chi^2$). Consequently, for predicting the drying kinetics of carrots in natural convection solar dryer the New Model 1 was found to be the best mathematical model with an $R^2$ = 0.999 for julienne, and 0.9986 for cylindrical cuts. In forced convection drying, the best suitable models were New Model 1 for julienne cuts ($R^2$ = 0.9987) and Diffusion approach for cylindrical cuts ($R^2$ = 0.9994). Finally, it has been observed that the $R^2$ values of New Model 1 and New Model 2 in all cases were greater than 0.99. Since there is a good agreement between theory and experimental data in this study, these developed models can provide a gain in the design of new solar dryers in the industry.

**Keywords:** Carrot drying, Drying kinetics, Mathematical modeling, Solar dryer

## Introduction

Sun drying is a food preservation technique that has been used for thousands of years. The aim of dehydration is to reduce the moisture content of agricultural products to a certain level, and to prevent them from spoiling within an accepted period of time.[1,2] However, it has some disadvantages such as being exposed to rain, hail and wind, contamination and dusting by insects and other animals which result in food loss and poor-quality products.[3]

Solar food dryers, which are a hygienic way compared to the traditional sun or shade drying methods, allow the drying parameters to be controlled, also provide a more uniform drying in a shorter time.[4,5] Today, these solar dryers are becoming attractive choices to alter industrial dryers due to the high energy costs, and the increased awareness of consumer orientation to clean energy products.

There are some studies in the literature on the drying and dehydration kinetics of carrots. Rubina *et al.* experimentally determine the thickness changes and shrinkage ratio of carrot cylinders during drying and rehydration processes.[6] Prakash *et al.* studied on the performance comparison of the drying characteristics of carrots using a solar cabinet, fluidized bed and microwave oven.[7] Béttega *et al.* did similar study by using microwave oven and vacuum drier, and analyzed how the driers influence the physical properties of carrot samples.[8] Some other studies exploring the thin layer drying of carrot are vacuum and ultrasonic vacuum drying[9], convective drying,[10,11] and infrared drying.[12]

While studies have been conducted on the drying kinetics of carrots using different dryers, there are only a few studies on the behavior of solar dried carrots. So, in order to contribute to the literature, carrot *(var. Danvers)* was examined as the product to be dried in this study. Ratti & Mujumdar developed a model to predict the batch drying performance of a packed bed of carrots. Shrinkage of food was considered in the model to reach more reliable predictions. The authors suggested that this model would be useful in developing a control system for batch solar dryers.[13] Tadesse *et al.* investigated the effects of pretreatments on nutritional quality and sensory acceptability of solar-dried carrot slices.[14]

According to Aghbashlo *et al.*, mathematical models should be defined accurately to estimate the drying behavior of biological materials.[15] There are

Author for Correspondence
E-mail: karasu@balikesir.edu.tr

plenty of research on modeling of drying kinetics in the literature. First attempts started in the 1990s, and Diamante & Munro investigated the solar drying of sweet potato slices with an indirect solar dryer. In this study, the drying curves were fitted with four different mathematical models, and it was found that the simplified form of the Fick's diffusion equation provided the best fit to the experimental data.[16] Yaldiz *et al.* conducted solar drying experiments for Sultana grapes and investigated the best mathematical equation to describe the solar drying curve of Sultana grapes.[1] A two-term model was selected among eight different models to represent the solar drying behavior of grapes.

Midilli & Kucuk studied on mathematical modeling of thin layer forced and natural solar drying of shelled and unshelled pistachios.[2] Non-linear regression analyses were done to determine the most suitable model, and the logarithmic drying model showed the best agreement with the experimental data obtained from twelve experiments. In 2002, Midilli *et al*. proposed a new drying model for single-layer drying.[17] They reported that this model adequately describes the drying kinetics, and it has gained a wide place in literature, and used in several studies.[3,10,18,19]

According to Diamante & Munro, there is a need for mathematical models that can be simulated in the development of solar dryer designs and in the operation of drying systems.[16] This study was mainly concerned with the development of new mathematical models of thin-layer drying kinetics of solar-dried carrots in both natural and forced convection solar dryers. First, the effects of the various drying airflow and the different cuts of carrots *(var. Danvers)* on drying parameters were investigated. Then, mathematical modeling of the drying kinetics was conducted by applying the five commonly used drying models and three newly introduced equations fitted to experimental data, and results were shared. It has been observed that the results obtained from experimental data are consistent with the newly introduced models as well as the other drying models in the literature.

## Materials and Methods

### Raw Material

Freshly harvested and organically grown orange carrots *(var. Danvers)* were provided by a local farmer. Samples were obtained for the experiment and kept in plastic bags at 4°C until the drying process.

Before drying, samples were washed under running water, the ends of carrots trimmed, and cut in two different shapes and sizes. The first one is the julienne shape which represents lengthwise slices (3 mm × 3 mm × 10 cm*),* and the other shape is the cylindrical shape that represents crosswise slices (5 mm thick, 2.5–3 cm). Thickness of 5 mm was chosen to prevent browning caused by long drying times in thick slices.[20] The process of peeling and cutting was done by the food processor. To inactivate peroxidase and color preservation, carrots were subjected to blanching for 90 seconds in a steam basket. Afterward, they were soaked instantly in an ice water bath to cool down for 60 seconds, then drained well, and removed excess water with a muslin cloth. Drying trays were prepared by spreading the carrots (single layer)*,* and not letting the pieces overlap.

The initial moisture content of blanched samples was determined by drying the sample in an electric drying oven at 105°C for 24 h[20] and found to be 89% on wet basis (w.b.), and 8.091 dry basis (d.b.) in g water per g dry matter ($g_w/g_{dm}$). The drying process was carried out in this oven until a constant weight was observed, and the equilibrium moisture content of carrot cuts was 0.136 (d.b.) which corresponds to 12% w.b. of dried product. Any product more than the target moisture level, can grow mold, and fail the quality of the finished product.[7] The drying experiment setup is presented in Fig. 1.

### Solar Dryer

A solar dryer was designed and constructed from stainless steel, as shown in Fig. 2. The entire structure is covered with insulating material to prevent heat losses and painted black to absorb the maximum amount of heat.

An airflow is created with two computer fans connected to the inlet of the collector. These DC fans are powered by a 20 W polycrystalline solar panel, as shown in Fig. 3. During the test phase of the dryer, it was observed that fans created a highly non-uniform distribution of heated air in the chamber. To fix this problem and create a uniform airflow, louvers that act like air distribution plates were mounted. So, the velocity and the direction of air being sent to the dryer were able to be controlled successfully, and a linear

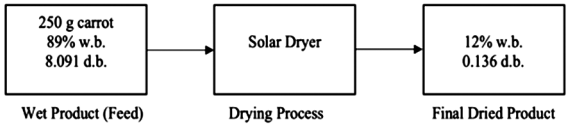


Fig. 1 — Schematic diagram of drying setup

Fig. 2 — Solar dryer

Fig. 3 — Two DC fans powered by a solar panel

air velocity of 0.5 m/s to the drying chamber was provided.

When the fans are used, drying is performed in the drying chamber with a constant airflow (0.5 m/s), and the dryer becomes a forced convection solar dryer. However, when the fans are not used, the airflow measured in the drying chamber varies, and the dryer acts like a natural convection solar dryer.

A rotating chimney cowl attached to the stovepipe was used to keep the airflow in the drying chamber continuous when the dryer is used as a natural convection dryer. This chimney acts like an aspirator and catches the wind causing it to rotate creating increased draw up the air.

A ten-sheets of black-painted fine-perforated metal fly screen was placed inside the collector (1200 mm × 700 mm × 250 mm) where the heat would be gained.

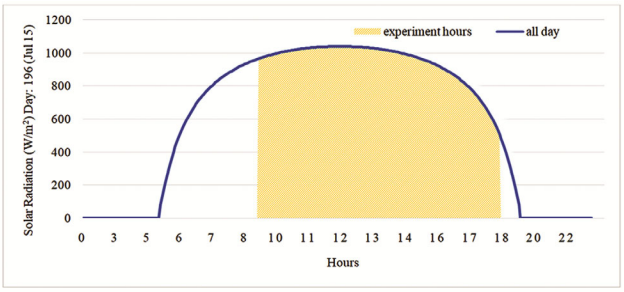


Fig. 4 — Solar radiation variation on the experiment day

The flat plate collector is faced south tilted at an angle of 39°, and 6 mm thick toughened glass was used as an absorber. A maximum of eleven wire mesh trays can be placed in the drying chamber (700 mm × 700 mm × 400 mm), but the experiments in this study were carried out on the first rack.

**Drying Carrots**

Carrot drying experiments were performed in Balikesir (39.7°N, 27.9°E) between 15–30 July 2020, an average of 11.6 hours of daylight a day. All experiments started at 9:00 and terminated at 18:00. The hourly variation of solar insolation for one representative solar drying experiment day is shown in Fig. 4. Here, the shaded area represents the solar radiation variation during the experiment hours, while the blue line shows the whole day. The summary of weather conditions on the 15$^{th}$ of July (Day: 196) is as follows, the max. solar insolation 1039 W/m$^2$ at 12:30, an average of 845.25 W/m$^2$, average ambient temperature and relative humidity 32.6°C and 38.9%, respectively.

In this study, the effects of the various airflow in the drying chamber and the different cutting shapes of carrots on drying parameters were investigated. Fresh carrots cut in different forms were placed on the mesh trays by ensuring that the carrots were placed in a single layer without overlapping. It was observed that a maximum of 250 g of carrots can be placed in each tray to meet this requirement, so each experimental setup was prepared accordingly (Fig. 5).

First, drying was carried out by natural convection without operating the fans, and the next day, the drying experiment was carried out with a constant airflow by operating the fans, and the results were compared. A total of 16 experiments (8 experiments with natural convection solar dryer and 8 experiments with forced convection) were carried out to ensure reproducibility of results, and the days with similar solar radiation were considered for the comparisons.

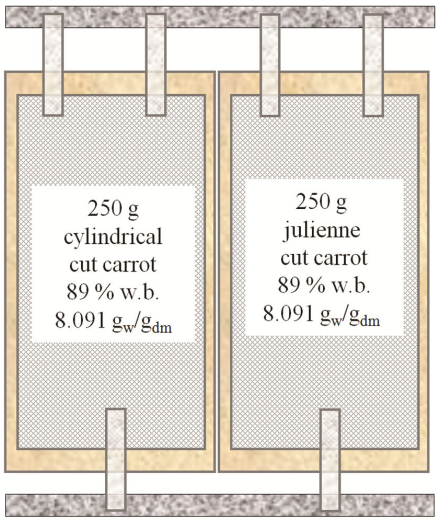


Fig. 5 — The position of the samples on trays at the rack in the drying chamber

Fig. 6 —The view of a load cell mounted on a rack

In Fig. 6 the placement of the samples on the tray placed on the first floor of the drying chamber is shown. As shown in Fig. 6, rack-mounted three load cells for both trays were used to monitor the change in weight during the drying process. The tare of the tray was subtracted from the total weight value taken from three load cells, and the weight measurement was recorded every 30 minutes.

**Data Collection and Uncertainties**

An Arduino program was written to monitor various data measurements which were recorded on an SD card every 30 minutes.

The collected data consists of the temperature and relative humidity of the drying chamber, collector, and ambient; weight change of the samples; and air velocity in the drying chamber and solar radiation. The instruments used in the experiments are given in Table 1.

Table 1 — Instruments used for the data collection

| Parameter | Instrument | Accuracy |
|---|---|---|
| i. Temperature and relative humidity data Logger *(inside the drying chamber)* | Testo 174H | ± 0.5°C and ± 3% rH |
| ii. Temperature *(inside the collector and ambient)* | DHT22 temperature sensor | ± 0.5°C |
| iii. Relative Humidity *(inside the collector and ambient)* | DHT22 humidity sensor | ± 2.0% rH |
| iv. Air velocity | Lutron YK-80AP | ± 2% + 0.2 m/s |
| v. Solar radiation | EKO MS80 pyrometer | ± 0.1 W/m² |
| vi. Weight Change | 1 kg capacity load cells | 0.0002 kg |

Table 2 — Independent variables for R analysis

| | Independent Variables | R (±) |
|---|---|---|
| i. Temperature | thermocouples, digital thermometer, connection points, reading | 0.350 |
| ii. Relative humidity | hygrometer, reading | 0.100 |
| iii. Mass loss | digital balance, reading, friction of tray | 0.269 |
| iv. Air velocity | anemometer, reading, air leaking | 0.173 |
| v. Moisture quantity | moisture analyser, reading | 0.014 |
| vi. Time | reading | 0.1 |

The uncertainties of the measured parameters are calculated through the root mean square error method that can be found a detailed explanation in Lakshmi *et al.*'s paper.[21] $\delta R$ is the uncertainty in the result of measured variables $(\partial x_1, \partial x_2, .. \partial x_n)$ and the uncertainty can be calculated by Eq. (1).

$$\delta R = \left\{ \left(\frac{\partial R}{\partial x_1}\delta x_1\right)^2 + \left(\frac{\partial R}{\partial x_2}\delta x_2\right)^2 + \cdots + \left(\frac{\partial R}{\partial x_n}\delta x_n\right)^2 \right\}^{\frac{1}{2}} \quad \ldots (1)$$

$$R(x_1, x_2, .., x_n) \quad \ldots (2)$$

Here in Eq. (2), R, the overall uncertainties of the experiment, indicates the function of different measured data $(x_1, x_2, \ldots x_n)$. While performing R analysis, various independent variables should be taken into account, and the variables considered in this study are presented in Table 2.

Based on these uncertainties of measured data, total uncertainty of moisture ratio ($R_{MR}$) is found 0.4847, and total uncertainty of drying rate ($R_{DR}$) is found 0.5254 from Eqs (3) – (4), respectively[22];

$$R_{MR} = \left\{\left(\frac{\partial MR}{\partial M_e}\delta R_{M_e}\right)^2 + \left(\frac{\partial MR}{\partial M_0}\delta R_{M_0}\right)^2\right\}^{\frac{1}{2}} \quad \ldots (3)$$

$$R_{DR} = \left\{\left(\frac{\partial DR}{\partial M_t}\delta R_{M_t}\right)^2 + \left(\frac{\partial DR}{\partial M_{t+\Delta t}}\delta R_{M_{t+\Delta t}}\right)^2 + \left(\frac{\partial DR}{\partial \Delta t}\delta R_{\Delta t}\right)^2\right\}^{\frac{1}{2}} \quad \ldots (4)$$

Here, $M_t, M_e$and $M_o$ indicate dry basis moisture at time *t*, the moisture equilibrium, and initial dry basis moisture, respectively.

**Mathematical Modeling**

The moisture ratio, $MR$, (dimensionless) was calculated as in Eq. (5);

$$MR = \frac{(M_t - M_e)}{(M_0 - M_e)} \quad \ldots(5)$$

However, dimensionless $MR$ was simplified to $\left(\frac{M_t}{M_0}\right)$since content of moisture of the drying air continuously fluctuated during the drying process.[1,10]

Drying rate, $DR$, (d.b.% in g/h) is the mass of moisture evaporated from the carrots per hour, and is calculated by Eq. (6);

$$DR = \frac{dM}{dt} = \frac{M_{t+\Delta t} - M_t}{\Delta t} \quad \ldots(6)$$

Drying is a kinetic process which is highly dependent on time. Various quasi-theoretical and empirical drying kinetics models developed by researchers to predict the drying behaviour of agricultural products are available in the literature.[23] In this study, eight different models listed in Table 3 were applied to find the best drying curve equation for all cases. The first five methods (Page, Lewis, Henderson and Pabis, Logarithmic and Diffusion Approach) are very common models in solar food drying literature.[1–3,15,18,24] The last three models developed considering the influence of drying factors or variables on drying coefficients and constants. These empirical equations, $\mathrm{MR}(a,b,c,n,k,t) = \left(\frac{M_t}{M_0}\right)$, are namely Growth Model, New Model 1 which was derived from logarithmic approach, and New Model 2 which was derived from diffusion approach are presented for the first time in this study.

Table 3 — Drying kinetics models

| Drying Model | Equation |
|---|---|
| Lewis | $MR = e^{(-kt)}$ |
| Page | $MR = \mathrm{e}^{(-kt^n)}$ |
| Henderson and Pabis | $MR = a\mathrm{e}^{(-kt)}$ |
| Logarithmic | $MR = a\mathrm{e}^{(-kt)} + \mathrm{c}$ |
| Diffusion Approach | $MR = a\mathrm{e}^{(-kt)} + (1-a)\mathrm{e}^{(-kbt)}$ |
| Growth Model | $MR = a(1 - e^{(-k/t)}))$ |
| New Model 1 | $MR = a\mathrm{e}^{(-kt^n)} + \mathrm{c}$ |
| New Model 2 | $MR = 1 - \mathrm{e}^{(-a/t) - bln(k) + c}$ |

These models include drying time as a variable, and the effect of drying conditions are expressed by the drying constants $(a, b, c, and\ n)$in these models. The coefficient $k$ is the measure of rate constant ($min^{-1}$), and *t* is time *(min)*. The larger the magnitude of $k$, the faster the moisture is being removed from food.

The coefficient of determination ($R^2$), the root mean square error (RMSE), and the mean square of the deviations ($\chi^2$) were calculated by Eqs (7) – (9) in order to determine the goodness of the fit. The highest value of $R^2$, and the lowest values of RMSE and $\chi^2$ are the indicators of the best fitted model. [2,21,23,25]

$$R^2 = \frac{\sum_{i=1}^{n}(MR_i - MR_{pre,i})\cdot\sum_{i=1}^{n}(MR_i - MR_{exp,i})}{\sqrt{\sum_{i=1}^{n}(MR_i - MR_{pre,i})^2\cdot\sum_{i=1}^{n}(MR_i - MR_{exp,i})^2}} \quad \ldots(7)$$

$$RMSE = \sqrt{\left[\frac{1}{N}\sum_{i=1}^{N}(MR_{pre,i} - MR_{exp,i})^2\right]} \quad \ldots(8)$$

$$\chi^2 = \frac{\sum_{i=1}^{n}(MR_{exp,i} - MR_{pre,i})^2}{N-n} \quad \ldots(9)$$

$MR_{exp,i}$ indicates the $i^{\text{th}}$ experimental moisture ratio, $MR_{pre,i}$ the $i^{\text{th}}$ predicted moisture ratio, $N$ the number of observations and, $n$ the number of constants.

## Results and Discussion

This section frames the results that have been revealed from drying experiments. First, drying factors that affected the drying parameters due to form of cuttings and various airflow evaluated. And then, the best fitted drying kinetic models and its parameters discussed.

**Factors that affect drying**

There are many factors that must be considered for successful drying. Some of them are related to the design of the dryer, and the others pertain to the characteristics of the product. The factors that are investigated in this study are shown in Fig. 7.

***Characteristics of Carrot***

Water removal depends on how far the water has to travel from the center of the product to its surface. So, the larger cuts tend to dry slower than the smaller ones.[26]

The final dried products can be seen in Fig. 8. The main difference between these cuts is the ratio of their surface area to volume which is higher in the case of

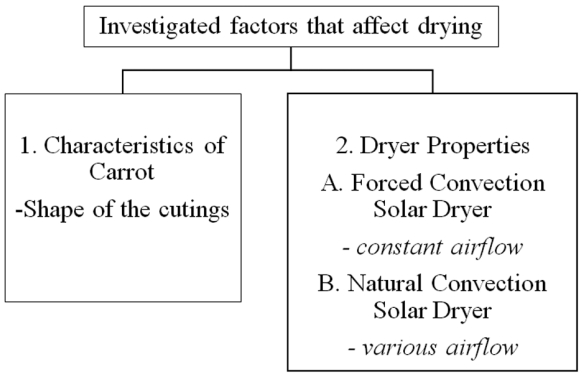


Fig. 7 — The investigated factors during drying process

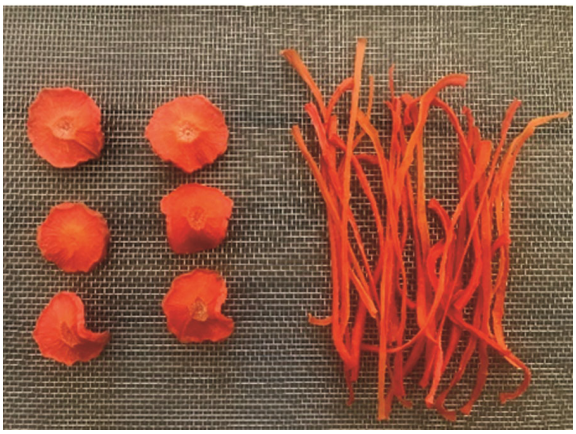

Fig. 8 — Dried carrots (on the left: cylindrical cut, on the right: julienne cut)

the julienne cut. Since the amount of surface area maximized, the rate of water removal observed to be high in julienne cuts comparing to cylindrical cuts.

The change of dry basis moisture content in $g_w/g_{dm}$ versus time in min at constant drying airflow is shown in Fig. 9. According to this graph, there is no warmup period for carrot cuts. The vertical lines at the beginning of the drying process indicate that there is a high rate of moisture in the carrot samples which leads a high rate of diffusion, which corresponds to constant drying rate period.

During this period, moisture was being removed from cylindrical and julienne cuts at a rate of 1.3527 and 1.6511 $g_w/g_{dm}$ per h, respectively. On the other hand, the horizontal lines at the end of the drying process indicate that as more water is evaporated, there is less moisture left in the samples which reduces the rate of moisture loss. This corresponds to falling rate of drying period, and it was found that during this period the moisture in carrots was lost at a rate of 0.1569 and 0.208 $g_w/g_{dm}$ per hour for cylindrical and julienne cuts, respectively.

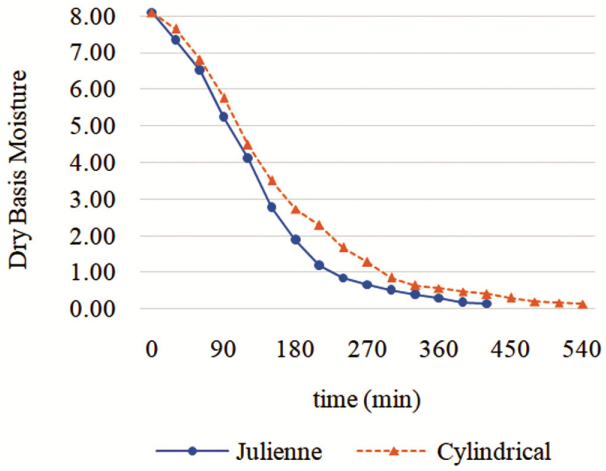


Fig. 9 — Dry basis moisture vs. time for julienne and cylindrical cuts at constant airflow

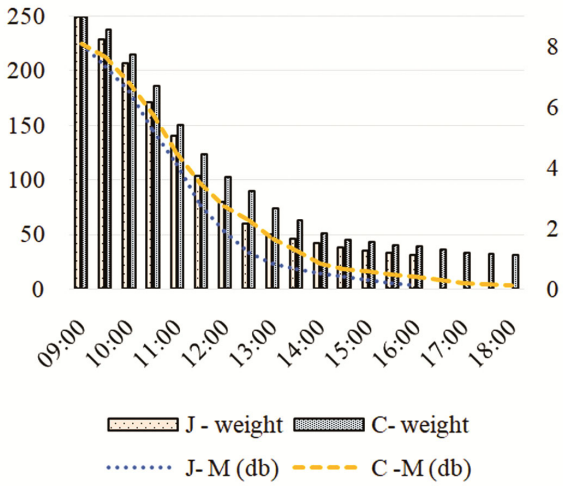


Fig. 10 — The variation of weight and dry basis moisture content changes in julienne (J) and cylindrical (C) cuts by time at constant drying airflow

The hourly variation of weight and corresponding moisture content of both cuts at constant drying airflow is given in Fig. 10. The drying process started 250 g of carrots with an initial moisture content of 8.091 (d.b.), ended when the final moisture content of 0.136 (d.b.) was reached.

According to this experiment, julienne cut carrots were observed to be dried completely in 420 min, the average temperature and relative humidity of the drying chamber during the test period were recorded as 45.3°C and 24.6%, respectively.

Cylindrical carrots, on the other hand, dried after 105 min compared to julienne cut carrots, and during the experiment the temperature and humidity of the drying chamber were measured to be 44.1°C and

25.7%, respectively. As stated in Bettega *et al.*'s study, the geometric shape of the carrot influences the drying kinetics, also they reported that cylindrical form is responsible for a slower drying.[8]

Additionally, drying rates were calculated for the experiment performed at various airflow in natural convection solar dryer. Similar to experiments with constant airflow, julienne cut carrots completely dried at 450 min, and finished the drying process 110 min earlier than cylindrical cuts. During the constant drying period, drying rates for cylindrical and julienne cuts were found to be 1.2517 and 1.3527 $g_w/g_{dm}$ per hour, respectively, while they were 0.1466 and 0.255 $g_w/g_{dm}$ per hour for the falling drying period.

Airflow is an important variable that affects the drying time.[13] In the drying experiments performed by natural convection, it was observed that the velocity of the drying air ranged from 0.16 m/s and 0.67 m/s, with an average of 0.34 m/s. When the drying behavior of the same cuts at different airflows was examined, it was found that the complete drying for Julienne cuts ended approximately 30 min before than the experiment at constant airflow, this value is approximately 15 min for cylindrical cuts.

In Fig. 11 the change in temperature and relative humidity at the constant airflow during the experiment is shown. Typically, temperature in the drying chamber increased rapidly during the first two hours, and decreased slowly during the last two hours, but it was relatively constant between these hours. As a result, based on drying time vs temperature, relative humidity and airflow data, it can be concluded that as the drying air temperature and airflow increases, the drying time and relative humidity decreases.

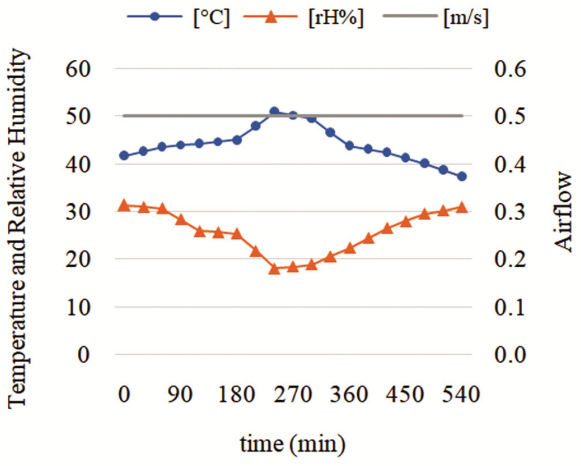


Fig. 11 —Temperature and relative humidity change at the drying chamber at 0.5 m/s

***Solar Dryer Properties***

During the drying experiments, temperature and relative humidity values of ambient, chamber and collector were collected, and the change of temperature and relative humidity during the experiment are presented in Figs 12 (a) & (b), respectively. As can be seen from these figures, temperatures and humidity changes collected from all three locations show similar trend in two different situations. Thus, it can be concluded that there was no significant difference in temperature and relative humidity for both cases.

**Modelling the Drying Kinetics**

In this study, five commonly used drying models and newly developed three models were compared to find the most fitted solar drying curve.

Moisture ratio data obtained from the experiments was plotted, and curved fitting application was utilized in MATLAB R2015a according to the Levenberg-Marquardt nonlinear optimization method. This algorithm, which combines the steepest descent and Gauss-Newton methods, is employed to determine the minimum of a multivariate function. If the solution is far from the correct one, the algorithm acts like the steepest descent, otherwise the algorithm behaves like Gauss-Newton. This method is widely used in solving nonlinear least squares problems.[27]

As mentioned earlier, the most suitable mathematical drying model was selected according to the highest $R^2$, and the lowest $\chi^2$ and RMSE criteria.

Moisture ratio vs time was plotted according to the data obtained from the drying experiments of different carrot cuts dried with various and constant drying airflow. Then, these data were fitted for all drying models, and the model coefficients, constants and goodness of fit values are given in Tables 4 & 5. Best fitted drying curves for all cases are presented in Figs (13) & (14).

The statistical results of fittings of julienne shaped carrots dried by two different dryers are summarized in Tables 4(a) – 5(a). It can be examined in Table 4 (a) that at constant airflow the New Model 1 fitted best with the experimental data compared with the other drying models, since the value of $R^2$ is the highest (0.9987), while the RMSE (0.01456) and $\chi^2$ (0.00233) are the lowest. According to the results of various airflow drying experiment of julienne cuts, as shown in Table 5 (a), New Model 1 fitted best with an $R^2$ of 0.999. Also, the following Page and New Model 2 performed very good fit with $R^2$ of 0.9973 and 0.9937, respectively. On the other hand, the Growth

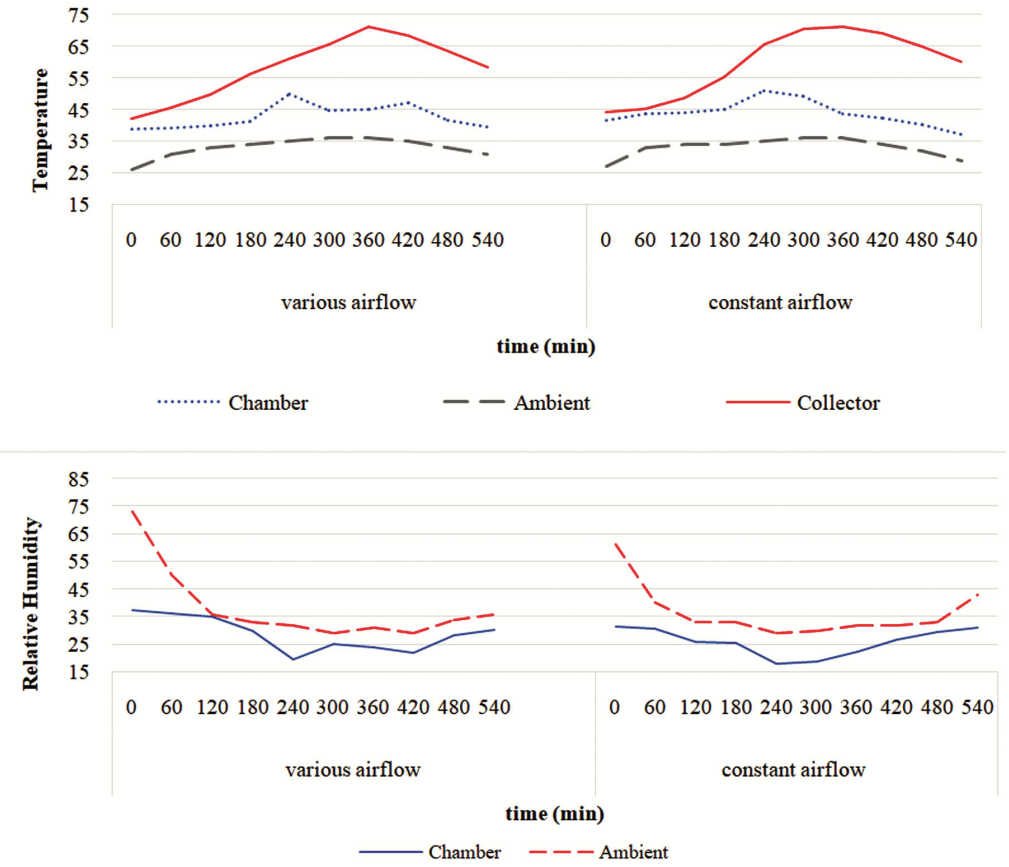


Fig. 12 — (a) Temperature, (b) Relative humidity change at different locations during the experiments

Table 4 — (a) Statistical results of julienne cut carrot drying models at constant airflow (forced convection solar dryer)

| Models | a | b | c | n | k | $R^2$ | RMSE | $\chi^2$ |
|---|---|---|---|---|---|---|---|---|
| New Model 1 | 0.9573 | 0.03029 | — | 1.813 | 0.0001246 | **0.9987** | **0.01456** | **0.00233** |
| Page | — | — | — | 1.641 | 0.0002765 | 0.9974 | 0.01865 | 0.00452 |
| New Model 2 | 178 | 2.581 | — | — | 0.3594 | 0.9936 | 0.03054 | 0.01119 |
| Logarithmic | 1.214 | — | −0.1228 | — | 0.006064 | 0.9773 | 0.05726 | 0.03934 |
| Diffusion Approach | −0.4139 | 0.9391 | — | — | 0.00754 | 0.9718 | 0.06382 | 0.04888 |
| Henderson and Pabis | 1.123 | — | — | — | 0.007886 | 0.9656 | 0.06773 | 0.05963 |
| Lewis | — | — | — | — | 0.007104 | 0.9505 | 0.07832 | 0.08588 |
| Growth model | 1.061 | — | — | — | 56.06 | 0.8968 | 0.11740 | 0.17920 |

model which also introduced in this paper generated the lowest $R^2$ values (0.8968 for constant airflow and 0.8982 for various airflow) which indicates the weakest fit among the other models. In Figs 13(a) & 14(a) the experimental and best fitted drying curves for julienne cuts are shown.

The drying parameters and the goodness of fit of the predicted curves to the experimental data of cylindrical cut carrots are shown in Tables 4 (b) – 5 (b), and best fitted curves are plotted, as in Figs 13 (b) –14 (b).When the results of cylindrical cuts dried under constant airflow are examined, Diffusion model with respect to the three variables used for the mathematical modeling gave the bestfit, with the highest $R^2$ (0.9994), and the lowest RMSE (0.009048) and $\chi^2$ (0.00131).

In fact, the $R^2$ values of all three models that follow (New Model 1, New Model 2 and Page) are greater than 0.999, that shows the perfect fit of the first four models in Table 4 (b). Meanwhile, when the various airflow drying results of the cylindrical cut carrots were examined, it is seen that the New Model 1 had the highest $R^2$ (0.9986), followed by New Model 2 (0.9935) and Logarithmic model (0.9849), as

Table 4 — (b) Statistical results of cylindrical cut carrot drying models at constant airflow (forced convection solar dryer)

| Models | a | b | c | n | k | $R^2$ | RMSE | $\chi^2$ |
|---|---|---|---|---|---|---|---|---|
| Diffusion Approach | -0.8774 | 0.4369 | — | — | 0.02081 | **0.9994** | **0.009048** | **0.00131** |
| New Model 1 | 0.9897 | 0.02363 | — | 1.515 | 0.0004251 | 0.9989 | 0.01209 | 0.00219 |
| New Model 2 | 164.6 | 1.507 | — | — | 0.1921 | 0.9979 | 0.01622 | 0.00421 |
| Page | — | — | — | 1.462 | 0.0005187 | 0.9977 | 0.01646 | 0.00461 |
| Henderson and Pabis | 1.123 | — | — | — | 0.006558 | 0.9801 | 0.04881 | 0.0405 |
| Logarithmic | 1.122 | — | -0.0081 | — | 0.006557 | 0.9801 | 0.04881 | 0.0405 |
| Lewis | — | — | — | — | 0.005897 | 0.9658 | 0.06226 | 0.06978 |
| Growth model | 1.067 | — | — | — | 65.49 | 0.9169 | 0.09979 | 0.16930 |

Table 5 — (a) Statistical results of julienne cut carrot drying models at various airflow (natural convection solar dryer)

| Models | a | b | c | n | k | $R^2$ | RMSE | $\chi^2$ |
|---|---|---|---|---|---|---|---|---|
| New Model 1 | 0.9578 | 0.02931 | — | 1.789 | 0.00014 | **0.9990** | **0.0123** | **0.0018** |
| Page | — | — | — | 1.621 | 0.00030 | 0.9973 | 0.0189 | 0.0049 |
| New Model 2 | 178.3 | — | — | — | 0.36 | 0.9937 | 0.0296 | 0.0114 |
| Logarithmic | 1.189 | — | -0.0957 | — | 0.00630 | 0.9774 | 0.0562 | 0.0410 |
| Henderson and Pabis | 1.122 | — | — | — | 0.00782 | 0.9682 | 0.0641 | 0.0576 |
| Diffusion Approach | 1.872 | 0.00599 | — | — | 0.00599 | 0.9585 | 0.0761 | 0.0753 |
| Lewis | — | — | — | — | 0.007066 | 0.9540 | 0.0746 | 0.0835 |
| Growth model | 1.062 | — | — | — | 55.71 | 0.8982 | 0.1149 | 0.1847 |

Table 5 — (b) Statistical results of cylindrical cut carrot drying models at various airflow (natural convection solar dryer)

| Models | a | b | c | n | k | $R^2$ | RMSE | $\chi^2$ |
|---|---|---|---|---|---|---|---|---|
| New Model 1 | 0.985 | 0.02581 | — | 1.54 | 0.00037 | **0.9986** | **0.0128** | **0.0024** |
| New Model 2 | 122.1 | 0.04592 | — | — | 0.05059 | 0.9935 | 0.0297 | 0.0132 |
| Logarithmic | 1.173 | — | -0.1029 | — | 0.00538 | 0.9849 | 0.0438 | 0.0308 |
| Henderson and Pabis | 1.119 | — | — | — | 0.00648 | 0.9783 | 0.0511 | 0.0444 |
| Lewis | — | — | — | — | 0.00585 | 0.9645 | 0.0635 | 0.0726 |
| Page | — | — | — | 0.0096 | 0.60630 | 0.9645 | 0.0654 | 0.0726 |
| Diffusion Approach | 0.255 | -0.3876 | — | — | 0.00585 | 0.9645 | 0.0674 | 0.0726 |
| Growth model | 1.067 | — | — | — | 66.17 | 0.9157 | 0.1007 | 0.1723 |

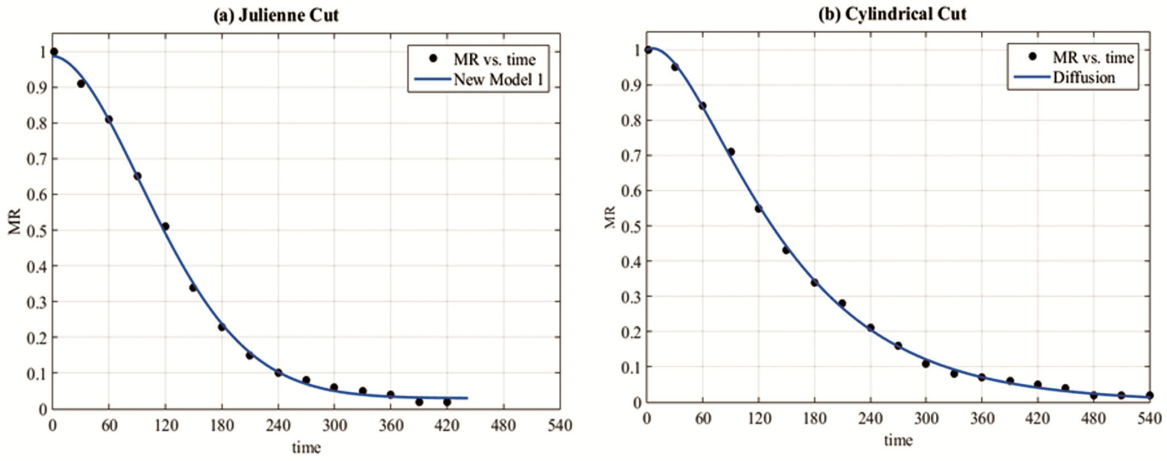


Fig. 13 — Best fitted drying curves of (a) julienne cut and (b) cylindrical cut at constant drying airflow

presented in Table 5 (b). Besides, the Growth model was the worst equation that predicted the drying curves of cylindrical cut carrots, and this model can be interpreted as the weakest fit of all models.

In summary, all drying curves were fitted with the eight models listed in Table 3. For all cases, all the mathematical models produced high $R^2$ (in the range of 0.8968 to 0.9994), which means all the models

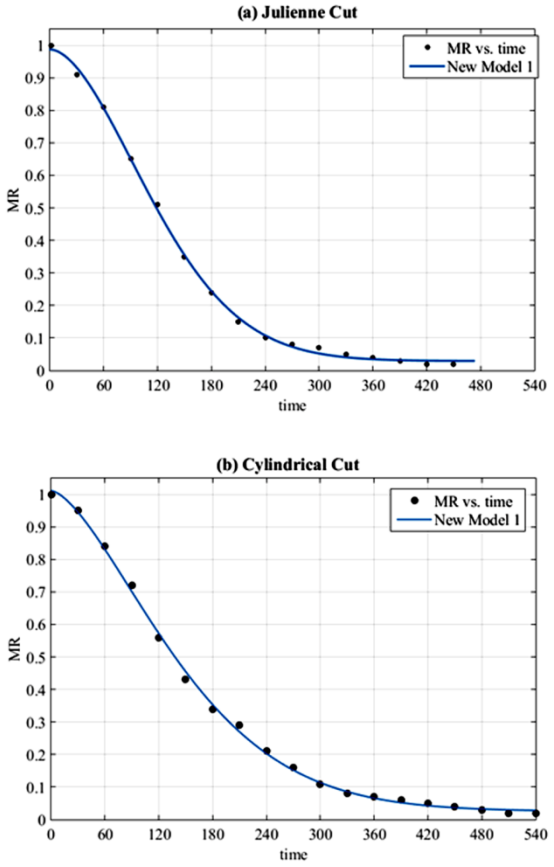


Fig. 14 — Best fitted drying curves of (a) julienne cut and (b) cylindrical cut at various drying airflow

satisfactorily fit the solar drying curves of carrots. But if a comparison needs to be made among all models, Growth model is the worst fit among all equations, regardless of the different airflows and shapes. This newly introduced model grossly overestimates the moisture ratio. However, the other equations proposed as New Model 1 and New Model 2 were perfectly suited for drying carrots in different shapes and airflow.

## Conclusion

In this study, the development of new mathematical models of thin layer drying behavior of carrots in natural and forced convection solar dryers has been studied. The solar drying experiments of two different sliced carrots at two different drying airflow were compared and the best mathematical models for each case were obtained. It can be concluded that the results obtained from the experiments carried out within the scope of this study are consistent with newly developed models as well as the frequently used thin layer drying models in the literature.

The following conclusions were drawn from the study:

1. Uneven distribution of air creates a lack of uniformity in the moisture of the dried carrots. In the first design of dryer, non-uniformity of airflow was observed when the fans spin. To fix this problem louvres were mounted, and a uniform flow was reached at all locations. So, in the experiments, all carrot pieces received same degree of exposure to the heated drying air.
2. The moisture removal rate during the constant drying rate period observed to be 1.3527 $g_w/g_{dm}$ per h for cylindrical, and 1.6511 for julienne cuts in constant airflow experiment, and1.2517for cylindrical and 1.3527 for julienne in various airflow experiments. Similar results were also observed during the falling drying period. It can be concluded that preparing carrots in julienne cuts increases the surface area while reducing its thickness, accordingly both of these actions were led to speeding up the rate of drying.
3. Drying rate periods were determined, both drying rates at falling and constant drying periods were calculated. The results show that the more moisture is removed, the rate of moisture removal gets slower. For example, in various airflow drying experiments for cylindrical cuts, the drying rate was calculated 1.2517 at the constant drying period and this value decreased to 0.1466 at the falling drying period.
4. Among the newly introduced models, named New Model 1 and New Model 2, fitted very well with the experimental data compared with the other well-known drying models. In fact, in 3 of the 4 cases, the New Model 1 provided the best fit by producing the highest $R^2$ (0.9987 for julienne at constant airflow, 0.9990 for julienne and 0.9986 for cylindrical cut at various airflow). Also, experimental data fitted very well to New Model 2, since the produced $R^2$ values were above 0.99 in all cases. However, the other new model introduced in this study named Growth Model resulted in the lowest $R^2$,the Growth model which also introduced in this paper generated the highest $\chi^2$ and RMS, and the lowest $R^2$ values (0.8968 for julienne cut and 0.9169 for cylindrical cut at constant airflow, 0.8982 and 0.9157at various airflow) for all cases.

The future scope of this study is to conduct further studies by drying different food stuffs in this dryer for the validation of the developed mathematical models

and to compare performance with a larger number of models.

**Acknowledgement:** This study was supported by Scientific Research Coordination Unit of Balikesir University under the project number BAP.2019/081. The author wishes to acknowledge the support received by Dr Ayse Ozdogan Dolcek and Dr Ilker Eren from Balikesir University.

## References

1 Yaldiz O, Ertekin C & Uzun H I, Mathematical modeling of thin layer solar drying of sultana grapes, *Energy*, **26** (2001) 457–465.

2 Midilli A & Kucuk H, Mathematical modeling of thin layer drying of pistachio by using solar energy, *Energy Convers Manag*, **44** (2003) 1111–1122.

3 Vijayan S, Arjunan T V & Kumar A, Mathematical modeling and performance analysis of thin layer drying of bitter gourd in sensible storage based indirect solar dryer, *Innov Food Sci Emerg Technol*, **36** (2016) 59–67.

4 Esper A & Mühlbauer W, Solar drying - An effective means of food preservation, *Renew Energy*, **15** (1998) 95–100.

5 Nourhène B, Mohammed K & Nabil K, Experimental and mathematical investigations of convective solar drying of four varieties of olive leaves, *Food Bioprod Process*, **86** (2008) 176–184.

6 Rubina T, Aboltins A, Palabinskis J & Jotautiene E, Study of drying and rehydration kinetics of carrot cylinders, *Eng Rural Dev*, **17** (2018) 1488–1493.

7 Prakash S, Jha S K & Datta N, Performance evaluation of blanched carrots dried by three different driers, *J Food Eng*, **62** (2004) 305–313.

8 Béttega R, Rosa J G, Corrêa R G & FreireJ T, Comparison of carrot (Daucus carota) drying in microwave and in vacuum microwave, *Brazilian J Chem* Eng, **31** (2014) 403–412.

9 Chen Z G, Guo X Y & Wu T, A novel dehydration technique for carrot slices implementing ultrasound and vacuum drying methods, *Ultrason Sonochem*, **30** (2016) 28–34.

10 Sonmete M H, Mengeş H O, Ertekin C & Özcan M M, Mathematical modeling of thin layer drying of carrot slices by forced convection, *J Food Meas Charact*, **11** (2017) 629–638.

11 Velescu I D, Ţenu I, Carlescu P & Dobre V, Convective Air Drying Characteristics for Thin Layer Carrots, *Food Sci Technol*, **70** (2013) 129–136.

12 Doymaz I, Infrared Drying Kinetics and Quality Characteristics of Carrot Slices, *J Food Process Preserv*, **39** (2015) 2738–2745.

13 Ratti C & Mujumdar A S, Solar drying of foods: Modeling and numerical simulation, *Sol Energy*, **60** (1997) 151–157.

14 Teferra T F, Abera S & Worku S, Nutritional and Sensory Properties of Solar-Dried Carrot Slices as Affected by Blanching and Osmotic Pre-Treatments, *Int J Food Sci Nutr Eng*, **5** (2015) 24–32.

15 Aghbashlo M, Kianmehr M H, Arabhosseini A & Nazghelichi T, Modelling the carrot thin-layer drying in a semi-industrial continuous band dryer, *Czech J Food Sci,* **29** (2011) 523–538.

16 Diamante L M & Munro P A, Mathematical modelling of the thin layer solar drying of sweet potato slices, *Sol Energy*, **51** (1993) 271–276.

17 Midilli A, Kucuk H & Yapar Z, A new model for single-layer drying, *Dry Technol*, **20** (2002) 1503–1513.

18 Hamdi I, Kooli S, ElkhadraouiA, Azaizia Z, Abdelhamid F & Guizani A, Experimental study and numerical modeling for drying grapes under solar greenhouse, *Renew Energy*, **127** (2018) 936–946.

19 Atalay H, Performance analysis of a solar dryer integrated with the packed bed thermal energy storage (TES) system, Energy, **172** (2019) 1037–1052.

20 Md Saleh R, Kulig B, Hensel O & Sturm B, Investigation of dynamic quality changes and optimization of drying parameters of carrots (Daucus carota var. laguna), *J Food Process Eng*, **43** (2019) 1–17.

21 Lakshmi D V N, Muthukumar P, Layek A & Nayak P K, Drying kinetics and quality analysis of black turmeric (Curcuma caesia) drying in a mixed mode forced convection solar dryer integrated with thermal energy storage, *Renew Energy*, **120** (2018) 23–34.

22 Özel Ö F, *Balkabağının farklı kurutma şartlarındaki kuruma karakteristiklerinin belirlenmesi*, MS Thesis, Selçuk University Institute of the Natural and Applied Sciences, Konya, Turkey, 2010.

23 Karthikeyan A K & Murugavelh S, Thin layer drying kinetics and exergy analysis of turmeric (Curcuma longa) in a mixed mode forced convection solar tunnel dryer, *Renew Energy*, **128** (2018) 305–312.

24 Yahya M, Design and performance evaluation of a solar assisted heat pump dryer integrated with biomass furnace for red chilli, *Int J Photoenergy* **2016** (2016) 1–14.

25 Akpinar E K, Drying of mint leaves in a solar dryer and under open sun: Modelling, performance analyses, *Energy Convers Manag*, **51** (2010) 2407–2418.

26 Mercer D G, *An Introduction to the Dehydration and Drying of Fruits and Vegetables* (University of Guelph, Ontario) 2014, 64–83.

27 Lourakis M, A Brief Description of the Levenberg-Marquardt Algorithm, *Matrix*, **3** (2005).